AIAA 81-0586R

Multiwall TPS—An Emerging Concept

John L. Shideler,* H. Neale Kelly,† Don E. Avery,* Max L. Blosser,* and Howard M. Adelman‡
NASA Langley Research Center, Hampton, Va.

This paper reviews some of the effort required to transform one thermal protection system concept, titanium multiwall, from a conceptual design to a practical working reality. Gradually, from continuing analytical and experimental studies, a fundamental understanding of the thermal and structural performance of the basic multiwall concept is evolving. In addition, radiant heat, wind-tunnel, vibration, acoustic, and lightning strike tests are being used to verify the performance of multiwall tiles under representative operating conditions, and flight tests of a large array of tiles are planned as part of an Orbiter experiments program. Results of the tests are being used to improve the design, and a mature technology is emerging. To date, research has focused on flat all-titanium multiwall configurations, which are limited to temperatures below 810 K (1000°F); however, the effort is being extended to include curved surfaces and higher temperature versions of the multiwall concept. Preliminary estimates indicate that these concepts, which offer the inherent durability of metallic systems, are mass competitive with the insulation system currently employed on the Space Shuttle Orbiter.

Nomenclature

BP	= body point
d	= distance from top surface
h	= height of thermal model
k_{eff}	= effective conductivity
OASPL	= overall sound pressure level
q	= net heat flux
T	= temperature
t	= time
T_A	= average temperature
T_l	= temperature of lower surface
T_s	= average upper surface temperature
T_u	= temperature of upper surface
ϵ	= emissivity

Introduction

IN a continuing effort to provide lightweight, durable thermal protection systems (TPS) for current and future space transportation systems, various metallic TPS concepts are being investigated.[1] One of the more promising systems under study is a family of concepts known collectively as multiwall.[2] To date, most of the efforts to verify these concepts have been concentrated on a titanium version intended for application in a moderate temperature range [590-810 K (600-1000°F)]. Design considerations for this concept are given in Ref. 2, and fabrication details are given in Ref. 3. The purpose of this paper is to provide an overview of efforts to evaluate the design and performance of the titanium multiwall TPS concept. These efforts include thermal and structural analyses and tests, wind-tunnel tests, lightning tests, and exposure to acoustic and vibrational environments.

Titanium Multiwall Tiles

The multiwall TPS concept is illustrated in Fig. 1. An array of discrete tiles are mechanically attached to the primary structure by bayonet-type tabs which are metallurgically bonded to the tile bottom surface. These tabs slide through clips mechanically attached to the primary structure. Each tab also slides through a clip which is bonded to the bottom surface of the adjacent tile. Nomex felt strips under the perimeter of the tile are compressed slightly when each tile is attached. The purpose of the strips is to block hot gas which otherwise might flow under the tile and to attenuate vibration. The attachment scheme permits differential thermal expansion between the tiles and the primary structure. Gaps between tiles are covered by the top and bottom lips of the tiles, and flow within the gaps is impeded by nesting of beaded close-out edges. The beaded close-out edges also accommodate differential thermal growth due to a temperature gradient through the tile thickness.

The interior of a tile, shown in Fig. 2, consists of multiple layers of superplastically formed dimpled sheets and flat septum sheets of titanium foil. These sheets are assembled in superplastically formed foil cover sheets which have scarfed edges and a lip on two sides which overhang adjacent tiles. The sheets are bonded into discrete tiles using a liquid interface diffusion (LID) bonding process.[3] In this process, the surfaces to be diffusion bonded are plated with a material which creates a eutectic solution with titanium when heated to 1214 K (1725°F). Subsequently, this material diffuses into the titanium which solidifies and forms a bond with properties comparable to the parent metal. The LID bonding process

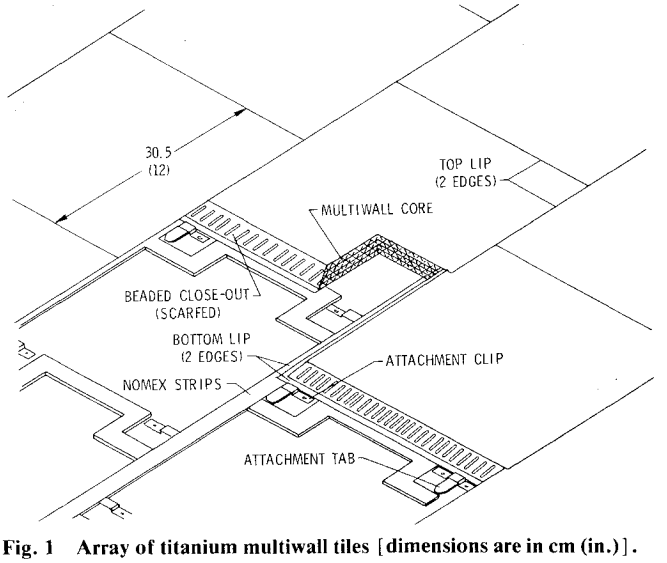

Fig. 1 Array of titanium multiwall tiles [dimensions are in cm (in.)].

Presented as Paper 81-0586 at the AIAA/ASME/ASCE/AHS 22nd Structures, Structural Dynamics and Materials Conference, Atlanta, Ga., April 9-10, 1981; submitted April 15, 1981; revision received Jan. 4, 1982.

*Aerospace Engineer, Aerothermal Loads Branch, Loads and Aeroelasticity Division.

†Assistant Head, Aerothermal Loads Branch, Loads and Aeroelasticity Division.

‡Aerospace Engineer, Multidisciplinary Analysis and Optimization Branch, Loads and Aeroelasticity Division.

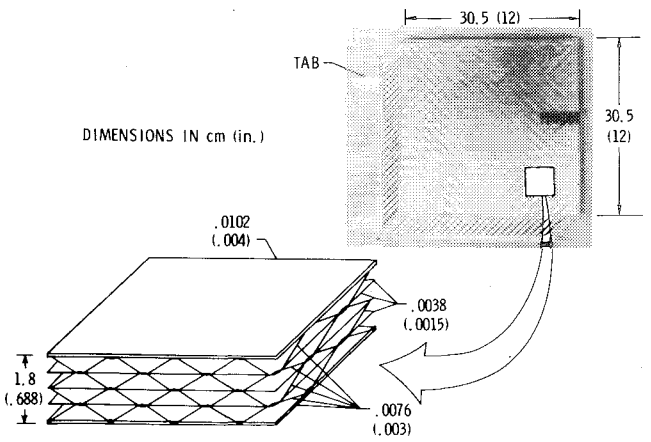

Fig. 2 Assembled multiwall tile [dimensions are in cm (in.)].

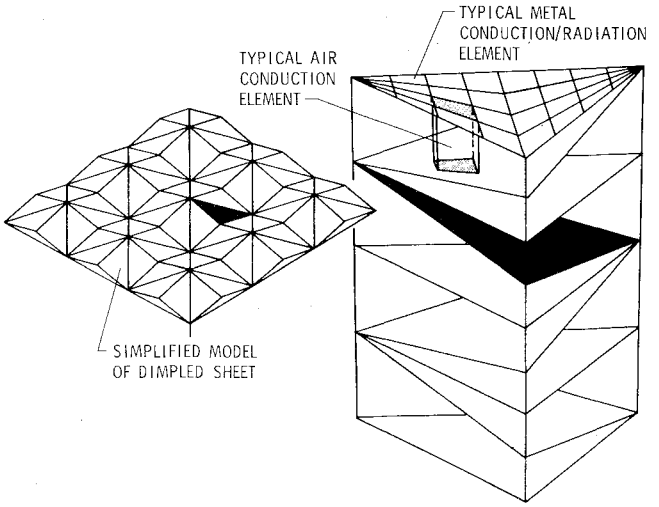

Fig. 3 Schematic of SPAR finite-element thermal model.

produces a metal-to-metal bond using much less contact pressure than that required for conventional diffusion bonding of titanium.

As indicated in Ref. 2, the multiwall concept impedes all three modes of heat transfer—conduction, radiation, and convection. The small contact area of the dimples and the long thin conduction path tends to minimize metal conduction; the multiple foil radiation shields impede heat transfer by radiation; and the small individual volumes created by the dimpled layers suppress air convection but permit air conduction.

Thermal Analysis and Tests

The inventor of the multiwall concept generated empirical equations based on available test data and engineering analysis to predict the thermal performance of multiwall TPS.[4] These equations, which were used in the preliminary design of multiwall tiles, have been modified to obtain better agreement with recently obtained experimental data. The modified empirical equations are presented in Ref. 2. To provide an analytical basis for understanding the multiwall heat transfer and to assess the empirical approach, a detailed analysis was performed using the SPAR finite-element analysis program.[5,6]

The complex geometry of the configuration required a very detailed model. A schematic of the SPAR model is shown in Fig. 3. The model contains 333 grid points located on 9 titanium sheets (5 horizontal and 4 inclined). The model contains 288 triangular and quadrilateral metal conduction elements, 264 solid elements which represent air conduction between sheets, and 544 radiation elements. The modeling of the multiwall concept takes advantage of symmetry and the finite-element model represents a basic repeating triangular prism cell which is cut out of the multiwall and is bounded by three planes of symmetry. The planes of symmetry were treated as adiabatic walls since there is zero net heat transfer through the planes. Temperature-dependent values for thermal conductivity for titanium and air were obtained from standard sources, and temperature-dependent emissivity of titanium was obtained from Ref. 3. Radiation view factors were computed by use of the general-purpose radiation computer program TRASYS II.[7]

The effective conductivity, k_{eff}, of the multiwall was obtained by 1) specifying the net heat flux at the upper surface q and the temperature at the lower surface T_l, 2) computing the temperature distribution in the model, and 3) calculating the effective conductivity from the equation

$$k_{\text{eff}}(T_A) = qh/(T_u - T_l)$$

Effective thermal conductivities from the empirical and finite-element analyses and experimental data from Ref. 3 are shown in Fig. 4 as a function of the average temperature T_A. A band representing the conductivity of low-temperature reusable surface insulation (LRSI-LI 900) is also shown for comparison.[8] The band is for a pressure range of 0.0001-1.0 atm. (The effective conductivity of titanium multiwall is essentially independent of pressure over this pressure range.) Finite-element results for the titanium multiwall are given for both an assumed constant emissivity of 0.4 and for measured emissivities which varied with temperature.[3] The empirical analysis used a constant emissivity of 0.4. The results from the finite-element analysis using measured emissivities are in fairly good agreement with the experimental data. The empirical analysis, while estimating the trends with temperature, tends to underestimate the importance of radiative heat transfer (especially at the higher temperatures) and slightly overestimates heat transfer by gas and metal conduction.

The indicated multiwall thermal conductivity is about twice the average conductivity of the basic Shuttle reusable surface insulation (RSI). However, the multiwall tile system can be made mass competitive with the Shuttle tile system because the effective density of the multiwall is lower and the heat transfer around the perimeter of the tiles is reduced by virtue of the covered gaps and the reduced gap-to-surface area of the larger multiwall tiles. For comparable thermal performance the multiwall tiles would be thicker, but not necessarily heavier, than the corresponding RSI tiles.[2]

Structural Analysis and Tests

Although the design study of Ref. 2 gives engineering approximations of the structural performance of multiwall, the complex geometry makes structural analysis difficult. Therefore, to provide a more fundamental understanding of the structural behavior, additional analytical and experimental studies have been undertaken. Central to this understanding is a knowledge of the extensional behavior of the dimpled sheets since the thinner flat sheets will buckle and be relatively ineffective in supporting compressive loads.

The geometry of the dimpled sheet, as indicated in Fig. 5, results in different extensional stiffnesses in the 0 and 45 deg directions. The SPAR structural analysis finite-element program[5] was used to calculate the extensional stiffness of the dimpled sheet in both the 0 and 45 deg directions. By taking advantage of conditions of symmetry, only small repeating areas of the dimpled sheet had to be modeled, as indicated by the shaded regions of Fig. 5. One-quarter of a single dimple was modeled in the 0 deg direction and one-quarter of two adjacent dimples was modeled in the 45 deg direction.

Superimposed triangular bending elements, each with half the material modulus, were used in the SPAR finite-element

models shown in Fig. 6 to represent the curved three-dimensional surfaces of the dimpled sheets. These elements were used to avoid inherent problems associated with warped quadrilateral elements (see, for example, Ref. 9). The boundaries of the model shown in Fig. 6 were treated as symmetry planes and therefore constrained to remain planar. Initially, three edges were fully constrained from lateral displacement, a uniform displacement was applied along the fourth edge as shown in the figure, and reactions in the direction of the displacement were calculated. The applied displacement and the reactions were used to calculate the extensional stiffness of the dimpled sheet. Using these extensional stiffnesses, the bending stiffness of one-, two-, and three-layer sandwiches with 0 and 45 deg dimple orientations were calculated using simple beam theory. In the latter calculations the flat sheets were assumed to be completely ineffective in compression. The calculated bending stiffnesses for specimens aligned with the 0 deg dimpled orientation agreed well with experimental results; however, the agreement for specimens aligned with the 45 deg dimple orientation was poor.

Consequently, to obtain a better understanding of the behavior of the dimple sheet, specimens with dimples oriented 0 and 45 deg to the inplane load were tested in tension. As expected, the dimpled sheet was found to be significantly less stiff than a flat sheet of the same thickness and was stiffer in the 0 deg direction than in the 45 deg direction, as indicated by the slope of the curves in Fig. 7. These tests also revealed that there was considerable lateral movement of the free edges of the specimens with the 45 deg dimple orientation (see Fig. 7) as the specimens deformed into a series of corrugations. Based on these observations, the dimpled sheets were reanalyzed with the lateral edges again constrained to be planar but, in addition, allowed to translate in the lateral direction. The change in boundary condition had little effect on the results for the 0 deg dimple orientation but significantly decreased the extensional stiffness of sheets with 45 deg orientation.

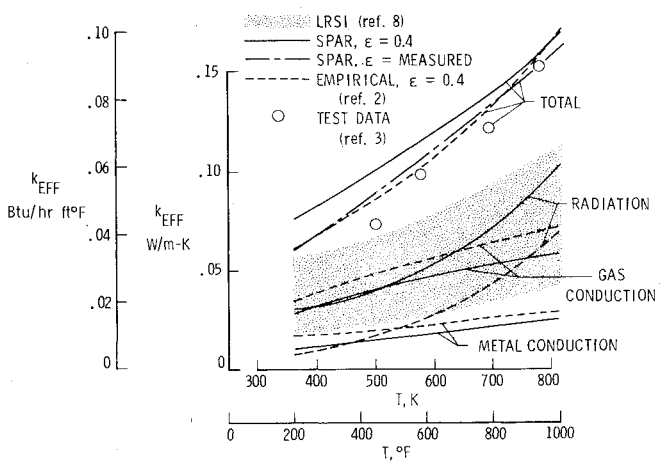

Fig. 4 Effective thermal conductivity of titanium multiwall.

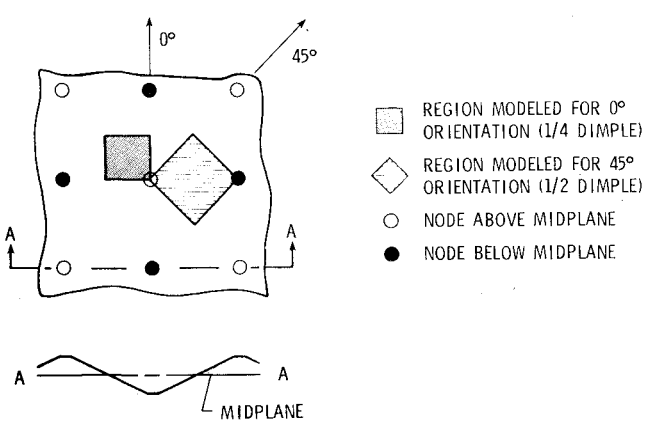

Fig. 5 Regions modeled for SPAR finite-element structural analysis of dimpled sheet.

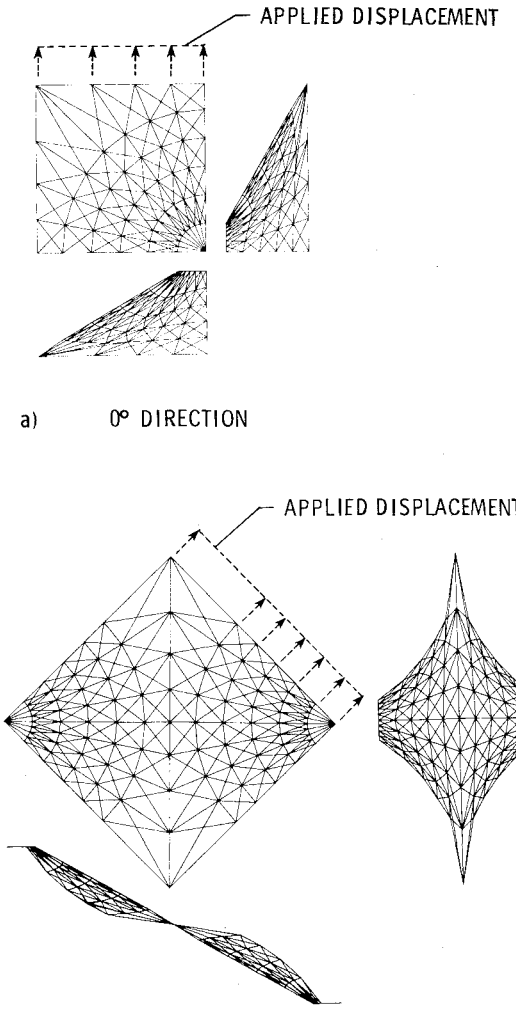

Fig. 6 SPAR finite-element structural models of dimpled sheet.

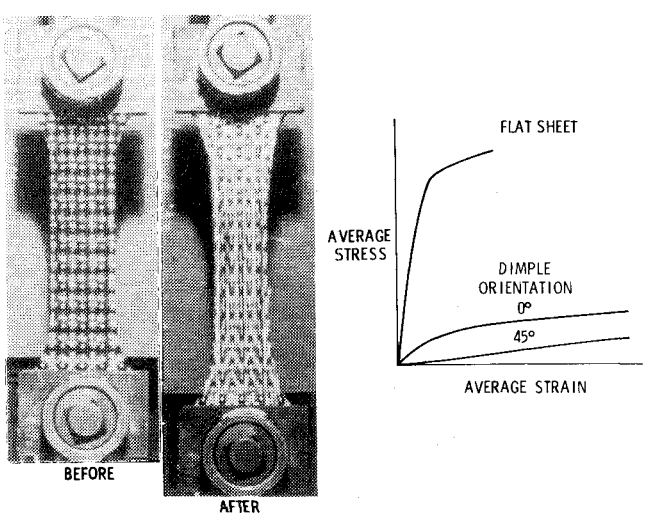

Fig. 7 Tensile tests of stainless steel dimpled sheets.

Table 1 Mass of RSI and multiwall test arrays

	Thickness, cm (in.)	Nominal mass, kg/m^2 (lbm/ft^2)	Attachment mass, kg/m^2 (lbm/ft^2) Nomex	Fasteners	Coating	Total mass, kg/m^2 (lbm/ft^2)
RSI	1.14[a]	1.64	0.35[b]	0.54[d]	0.81	3.34
	(0.45)[a]	(0.337)	(0.072)[b]	(0.110)[d]	(0.165)	(0.684)
Multiwall	1.75	2.64	0.07[c]	0.83[e]	0.10	3.64
	(0.688)	(0.541)	(0.014)[c]	(0.170)[e]	(0.02)	(0.745)

[a] Defined by Shuttle outer mold-line fairing requirements. [b] Covers total surface area, $t = 0.41$ cm (0.160 in.). [c] 2.54 cm (1 in.) wide strips, $t = 0.48$ cm Wide strips 2.54 cm (1 in.) $t = 0.48$ cm (0.190 in.). [d] Two RTV bond layers, each $t = 0.02$ cm (0.0075 in.). [e] Includes clips, tabs, and doublers.

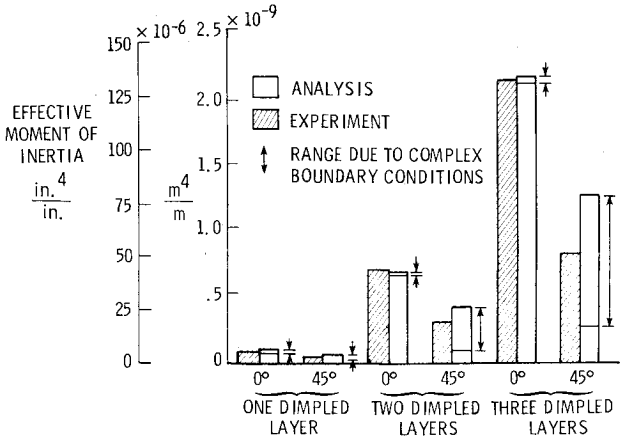

Fig. 8 Effective bending moments of inertia.

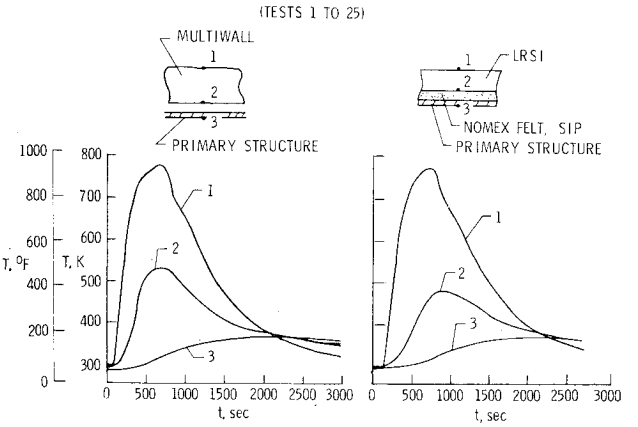

Fig. 9 Radiant heating cyclic tests—heating distributions through models (tests 1-25).

The influence of the variation in extensional stiffness of the dimpled sheets on the bending stiffness of one-, two-, and three-layer multiwall sandwiches is shown in Fig. 8 as an effective bending moment of inertia. In the 0 deg direction the calculated bending stiffnesses are in good agreement with experiment, and the choice of boundary conditions for the lateral edgewise displacement causes very little difference. In the 45 deg direction the calculated results, which bound the problem, bracket the experimental results. It is apparent that, in these uniaxial bending tests, the dimpled sheets in the multiwall sandwiches are partially restrained in the lateral direction by the flat sheets. It also appears that there are interactions between the flat sheets and the dimpled sheets not normally encountered with sandwich structures and that biaxial loading would undoubtedly alter the structural behavior. Thus, in summary, although a fundamental understanding of the structural mechanics of multiwall is emerging, continued study is required to improve the analysis and to develop and confirm parametric data so that the stiffnesses of multiwall with different geometric proportions can be calculated.

Radiant Heating Cyclic Tests

A two-tile array of multiwall tiles and a comparable area of low-temperature reusable surface insulation (LRSI-LI 900) were subjected to cyclic radiant heat in the Johnson Space Center Building 13 Radiant Heating Facility. The purpose of these tests was to evaluate the cyclic thermal performance of the multiwall and to provide a direct comparison with the performance of the insulation system currently employed on the Shuttle Orbiter. Both insulation systems were mounted on aluminum plates representative of the local thermal mass of the Shuttle structure. A comparison of the test arrays is given in Table 1. The thickness of the multiwall tiles was designed for the thermal requirements at body point 3140, but the thickness of the LRSI tiles was 60% greater than that required for thermal design [which was 0.71 cm (0.28 in.)] because of Shuttle Orbiter outer mold-line fairing requirements. Even so, the multiwall tiles were thicker because, as previously discussed, the conductivity of multiwall is higher than the conductivity of LI-900. The total mass of the multiwall system was 9% greater than the LRSI system. The tiles were subjected to 25 temperature and pressure cycles representative of conditions at body point 3140 during trajectory 14414.1C, the baseline design trajectory for the Shuttle.

Typical results for the two insulation systems are shown in Fig. 9. The performance of the insulation systems appears to be the same since the peak structural temperature beneath each system is the same. Each maintained the primary structure well below the maximum allowable temperature of 450 K (350°F). The results indicate that the thermal design of the multiwall system is conservative since it performed in the same way as the LRSI system which was 60% thicker than that required to meet the thermal requirements.

There was no significant change in the thermal performance of either system over the entire 25 cycles. Except for a slight curling of the overhanging edge between multiwall tiles and flaking of the thermal paint on the multiwall tiles which was unintentionally not cured before testing, there were no ill effects despite the fact that the insulations had been exposed to elevated temperatures for over 17 h.

Aerothermal Tests

A nine-tile array of multiwall tiles was subjected to radiant heating tests and combined radiant-heating/aerothermal tests in the Langley Research Center 8-ft High-Temperature Structures Tunnel (HTST). For these tests, the array shown in Fig. 10 was attached to an aluminum panel that was representative of the thermal mass of the Shuttle structure and mounted in the panel holder shown in Fig. 11. The tiles were staggered to avoid long, continuous gaps between tiles. In a typical test, the array was radiantly heated (following the temperature profile to the maximum temperature used for the tests of the two-tile array) before being inserted into the aerothermal environment of the tunnel. Flow conditions in the tunnel simulated the maximum temperature conditions

associated with this temperature profile. In addition to the heating environment, the wind tunnel imposed an acoustical load of 163 dB which, as shown in Fig. 12, was slightly higher but similar in frequency content to the design conditions expected at the reference body point.

During the initial radiant heating tests, significant debonding occurred between the top face sheet and the underlying dimpled sheet. This problem was not encountered with the two-tile array which was exposed to a similar thermal environment; furthermore, the debonding occurred mainly on the edge tiles which were partially restrained from thermal growth by the ceramic surface of the panel holder which surrounded the wind-tunnel array. Therefore, it is felt that unrealistic boundary conditions greatly contributed to the debonding problem. Surface debonding was repaired by spot welding (the tiles were not removed from the panel holder for repairs) and the array was subjected to seven radiant-heating tests and eight combined radiant-heating/aerothermal tests which included a total aerothermal exposure time of 294 s. Photographs in Fig. 13 show the center tile and the surrounding tiles of the nine-tile array before and after the tests. The wrinkles on the surface of the tiles were caused by an initial fabrication development problem and are not the result of testing. Although the array appears essentially the same before and after the tests, detailed inspection of the disassembled array revealed curling of the overhanging edge (similar to, but more severe than that encountered with the two-tile array) and five hairline cracks, all of which were on one of the boundary tiles which was adjacent to the ceramic surface of the panel holder.

These tests identified minor design changes to be incorporated in future designs to improve the fabrication and structural performance of the bonded joints. These changes include 1) slightly larger contact nodes, 2) alignment of tiles in an unstaggered manner to allow edge deflections of adjacent tiles to be more compatible, 3) use of stronger Ti 6Al-2Sn-4Zr-2Mo alloy in place of Ti 6A1-4V, and 4) a "stepped" edge closure to allow bonding fixtures to improve contact of the bond joints in the overhang region (this stepped edge closure was subsequently changed to a vertical beaded edge closure to avoid interference between panels due to thermal deformations).[10]

The aerothermal tests showed no evidence of localized convective heating in the gaps between tiles due to hot-gas ingress. Figure 14 shows typical maximum temperature distributions down the edge of a tile where gap flow would impinge if it were present. The temperatures are normalized by the average of the maximum surface temperature T_s measured at the two locations shown. Comparison of the maximum temperatures for radiant heating only with temperature from the aerothermal tests indicate an absence of any significant hot-gas ingress.

Vibration and Acoustic Tests

A tile was subjected to vibration tests on a shaker table at levels of 10, 20, and 31 Grms for 485 s per level. These tests, which were conducted for each of the three principle axes, approximate the severe portion of the vibration environment for 25 Shuttle missions (with a scatter factor of 4). At the end of the test, one hairline crack in the tile closeout adjacent to an attachment tab was detected. While this does not denote a serious problem, additional tests will be required to determine tile life.

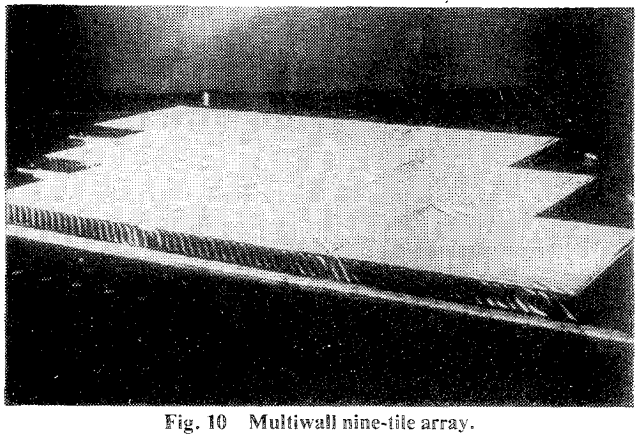

Fig. 10 Multiwall nine-tile array.

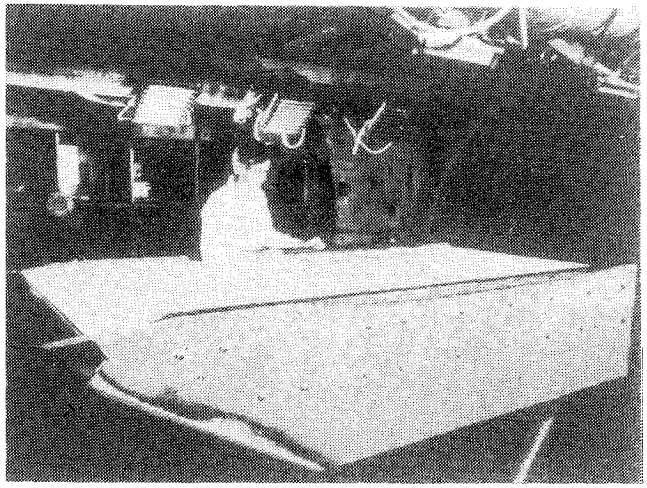

Fig. 11 Multiwall nine-tile array installed in Langley 8 ft High Temperature Structures Tunnel (Mach 7).

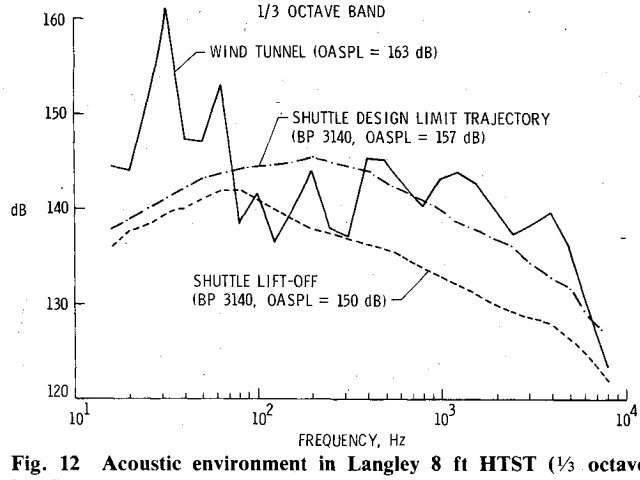

Fig. 12 Acoustic environment in Langley 8 ft HTST (⅓ octave band).

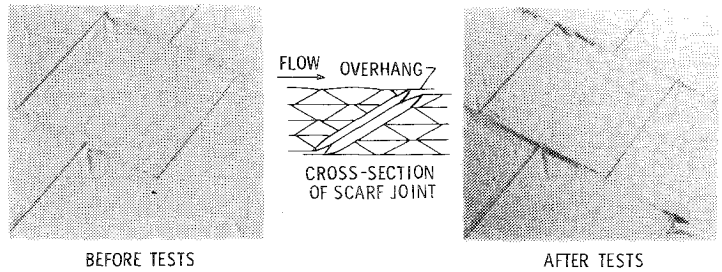

- 7 RADIANT HEATING CYCLES
- 8 AEROTHERMAL TESTS; TOTAL EXPOSURE TIME = 294 sec
- MINOR DESIGN AND FABRICATION MODIFICATIONS REQUIRED FOR SCARF/OVERHANG REGIONS

Fig. 13 Multiwall nine-tile array before and after testing in 8 ft High Temperature Structures Tunnel.

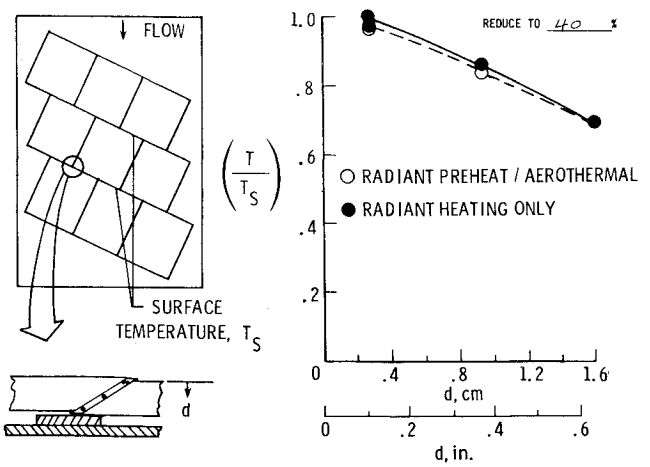

Fig. 14 Maximum gap temperatures with and without aerothermal flow.

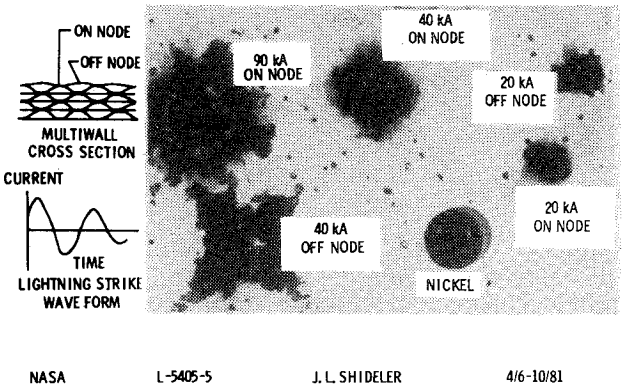

Fig. 15 Simulated lightning strikes on titanium multiwall.

A multiwall TPS tile was subjected to a series of exploratory sonic fatigue tests by Rohr Industries in a "progressive-wave tube" facility. The panel was exposed to random (Gaussian) noise on one surface at grazing incidence. The acoustic loading was representative of broadband jet or rocket exhaust noise. After preliminary tests to identify resonant frequencies and damping ratios, the tile was exposed to broadband random loading at 157 dB for 1.5 h. This time corresponds to approximately 40 missions (with a scatter factor of 4) at the design limit condition for Shuttle body point 3140 (see Fig. 12). Since no structural damage occurred, the tile was exposed to 161 dB. A face sheet failure occurred after 0.6 h when bond nuggets pulled out over a surface area of about 96 cm^2 (15 $in.^2$) near the center of the tile. Although more extensive tests are required to reach firm conclusions, these tests imply that the resistance of multiwall to acoustic fatigue will be acceptable for space transportation system application.

Lightning Strike Tests

A segment of a titanium multiwall tile was subjected to simulated lightning strikes of varying intensities in the Langley Research Center Lightning Simulation Test Facility. The wave form of the simulated lightning strike, shown on Fig. 15, was a lightly damped sinusoidal oscillation. At intensities representative of average lightning strikes (20-40 kA peak currents), only superficial damage occurred. At the higher of the two intensities (40 kA peak current), a strike midway between the nodes joining the skin to the underlying dimpled sheet produced a small burnthrough in the outer 0.0120 cm (0.004 in.) thick skin. A strike of 90 kA peak current, greater than 93% of naturally occurring lightning strikes, caused a crater with a diameter at the upper surface

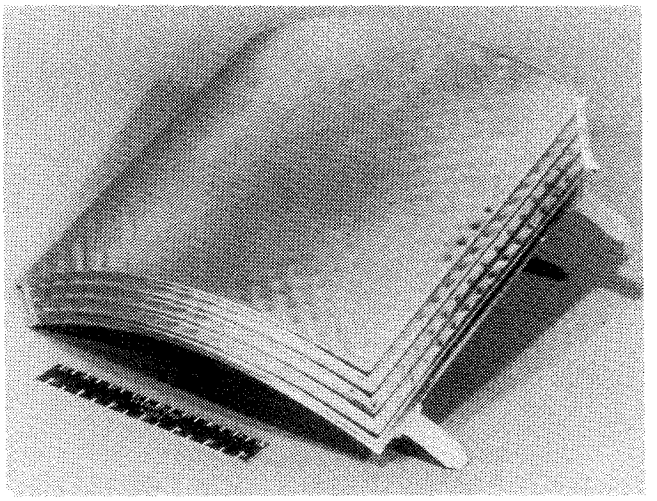

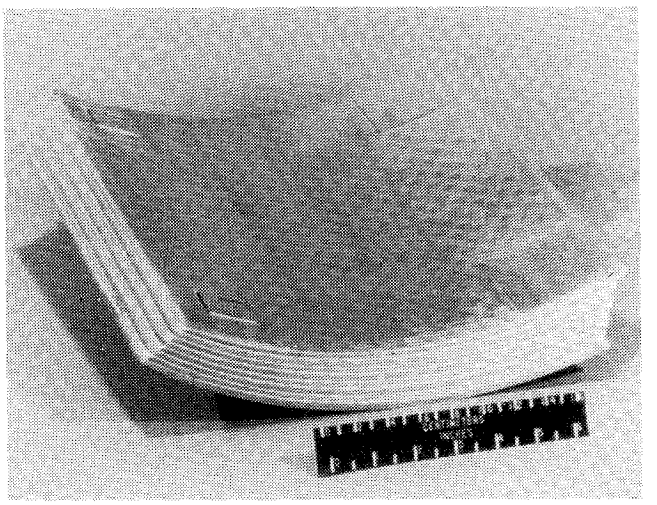

Fig. 16 Curved titanium multiwall tile, 30.5 cm (12 in.) radius.

about the size of a nickel that penetrated all but the bottom two layers. For comparison, a 1979 article[11] indicates that "The [current RSI-900] TPS can withstand 50,000 amperes with only surface cracking damage, but with a 100,000 ampere strike, two or three tiles may be blown off."

If damage due to lightning is not aggravated by airflow, the temperature of the structure under a damaged section of multiwall would not be significantly increased because the additional heat transfer through the locally damaged area would be readily dissipated by the high lateral conductivity of the aluminum structure. However, wind-tunnel tests will be required to determine if a tile damaged by lightning can withstand the entry aerothermal environment.

Fabrication Development

Titanium multiwall development has been extended to include the fabrication of a curved tile. The successfully fabricated tile, shown in Fig. 16, has an inner radius of 30.5 cm (12 in.). With this radius, which is a more severe curvature than the majority of surfaces on large spacecraft, the pitch of the dimples in different layers had to be varied so that the dimples would be aligned in the curved assembly. The dimpled sheets were formed in the flat condition and layed up in a curved bonding fixture with face sheets which had previously been superplastically formed in a curved die. For less severe curvature it may be possible to bond a tile in the flat condition and then form it into a curved tile. The tile shown in Fig. 16 was fabricated from Ti 6Al-4V and incorporates the design modifications which evolved from experience with the wind-

tunnel array, i.e., stepped edge closures and increased contact node size. Although most future structural and thermal testing will be with flat tiles, ultimately some wind-tunnel testing of curved surfaces will be required to evaluate possible heating in gaps between tiles where high surface pressure gradients exist.

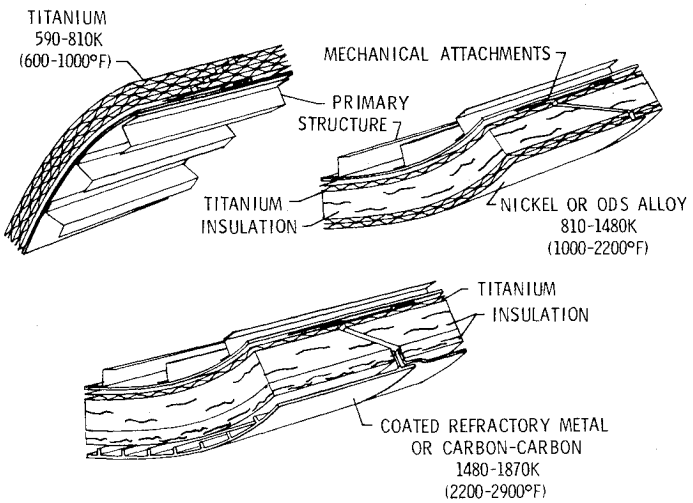

Fig. 17 Multiwall thermal protection system concepts.

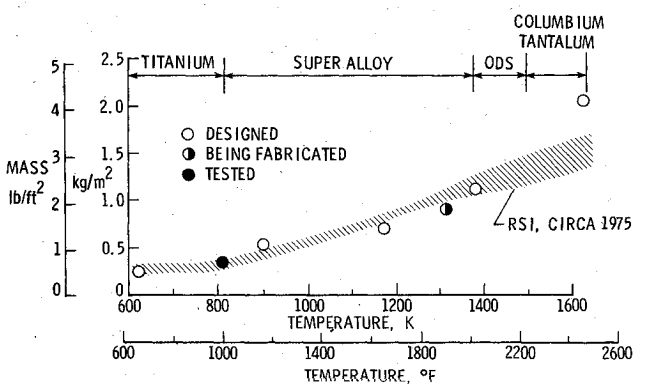

Fig. 18 Unit mass of multiwall concepts sized for Shuttle application.

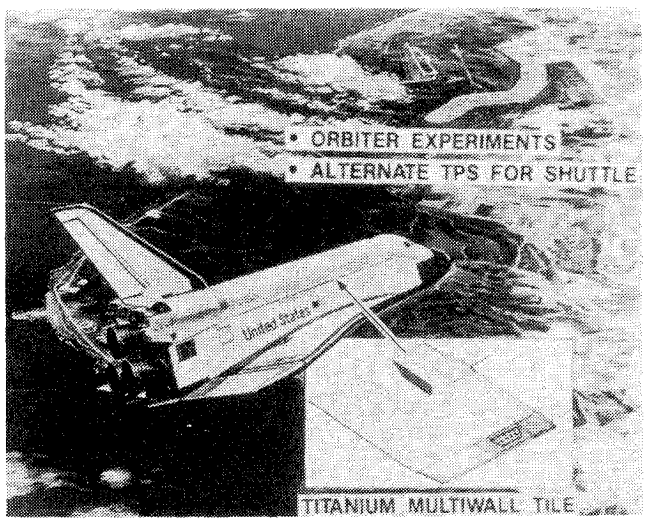

Fig. 19 Potential titanium multiwall applications.

Advanced Multiwall Concepts

Results of the analyses and tests of the all-titanium concept described herein for surface temperature up to about 810 K (1000°F) are being used to guide the design and fabrication of advanced multiwall concepts for higher surface temperature. The titanium concept and two advanced concepts are shown in Fig. 17. Arrays of the nickel alloy sandwich concept, which has fibrous quartz insulation in the center of the tile, are being fabricated for subsequent testing. This concept has an Inconel 617 outer sandwich fabricated as either a multiwall sandwich (shown in the figure) or as a honeycomb sandwich (not shown). Oxide dispersion strengthened (ODS) materials are also being considered for this concept to extend the use temperature range. Designs for even higher surface temperatures using coated refractory alloys and advanced carbon-carbon concepts[2] are being studied. The outer skin for the concepts are waffle or rib-stiffened to allow for ease in fabrication and coating.

Preliminary mass estimates for these concepts are shown in Fig. 18 compared with a band which represents the mass of RSI estimated in 1975. The temperature boundaries separating material systems are approximate. The solid symbol represents the all-titanium concept, and the half-solid symbol represents the superalloy concept currently being fabricated. These concepts appear to be mass competitive with the insulation system currently in use on the Shuttle Orbiter.

Continuing Development

A Shuttle Orbiter experiment (OEX) is planned in which approximately 2.3 m^2 (25 ft^2) of multiwall TPS will be placed on the side of the fuselage (see Fig. 19) to expose the tiles to the complete Shuttle operations environment and to find any problems associated with incrementally replacing the RSI tiles with metallic TPS. In support of this program, an array of 12 titanium multiwall tiles are being fabricated for testing in the Langley 8-ft HTST. These tiles will incorporate the design changes identified in the earlier tests previously discussed. In a separate study,titanium multiwall is one of the concepts being considered in Contract NAS1-16302, "An Assessment of Alternate Thermal Protection Systems for the Space Shuttle Orbiter," a study being conducted by Rockwell International Space Division for the Langley Research Center.

Conclusions

This paper reviews some of the effort required to transform one thermal protection system concept, titanium multiwall, from a conceptual design to a practical working reality. Gradually, from continuing analytical and experimental studies, a fundamental understanding of the thermal and structural performance of the basic multiwall concept is evolving. In addition, radiant heat, wind-tunnel, vibration, acoustic, and lightning strike tests are being used to verify the performance of multiwall tiles under representative operating conditions, and flight tests of a large array of tiles are planned as part of the Orbiter experiments program. Results of the tests are being used to improve the design, and a mature technology is emerging. To date, research has focused on flat all-titanium multiwall configurations, which are limited to temperatures below 810 K (1000°F); however, the effort is being extended to include curved surfaces and higher temperature versions of the multiwall concept. Preliminary estimates indicate that these concepts, which offer the inherent durability of metallic systems, are mass competitive with the insulation system currently employed on the Space Shuttle Orbiter.

References

[1] Bohon, H.L., Shideler, J.L., and Rummler, D.R., "Radiative Metallic Thermal Protection Systems—A Status Report," *Journal of Spacecraft and Rockets*, Vol. 14, Oct. 1977, pp. 626-631.

[2] Jackson, L.R. and Dixon, S.C., "A Design Assessment of Multiwall, Metallic Stand-Off, and RSI Reusable Thermal Protection Systems Including Space Shuttle Applications," NASA TM 81780, April 1980.

[3] Blair, W., Meany, J.E. Jr., and Rosenthal, H.A., "Design and Fabrication of Titanium Multi-Wall Thermal Protection System (TPS) Test Panels," NASA CR 159241, Feb. 1980.

[4] Jackson, L.R., Davis, J.G. Jr., and Wichorek, G.R., "Structural Concepts for Hydrogen Fueled Hypersonic Airplanes," NASA TN D-3162, Feb. 1966.

[5] *SPAR Structural Analysis System Reference Manual,* Vol. 1, NASA CR 158970-1, Dec. 1978.

[6] *SPAR Thermal Analysis Processors Reference Manual, System Level 16,* NASA CR 159162, Oct. 1978.

[7] Jensen, C.L. and Gable, R.G., "Thermal Radiation Analysis System (TRASYS II), User's Manual," NASA CR 159273-1, June 1980.

[8] Ebbesmeyer, L.H. and Christiansen, H.E., "Silica Heat Shield Sizing," NASA CR-151962, 1975.

[9] Robinson, J.C. and Blackburn, C.L., "Evaluation of a Hybrid, Anisotropic, Multilayered, Quadrilateral Finite Element," NASA TP-1236, Aug. 1978.

[10] Avery, D.E., Shideler, J.L., and Stuckey, R.N., "Thermal and Aerothermal Performance of a Titanium Multiwall Thermal Protection System," NASA TP-1961, 1981.

[11] Amsbary, M.S., Read, G.R., and Griffin, B.L., "Lightning Protection Design of the Space Shuttle," FAA-RD-79-6, 1979.